Phase transition of dissociatively adsorbed oxygen on Ag(001)

M. Rocca,* L. Savio, L. Vattuone, U. Burghaus,[†] V. Palomba, N. Novelli, F. Buatier de Mongeot, and U. Valbusa
Istituto Nazionale per la Fisica della Materia, and Centro di Fisica delle Superfici e delle Basse Temperature del CNR,
Dipartimento di Fisica, via Dodecaneso 33, 16146 Genova, Italy

R. Gunnella
Istituto Nazionale di Fisica della Materia and Dipartimento di Fisica, Camerino, Italy

G. Comelli,[‡] A. Baraldi, S. Lizzit, and G. Paolucci
Sincrotrone Trieste, 40100 Trieste, Italy

We show that dissociative oxygen adsorption on Ag(001) induces below room temperature a missing row $2\sqrt{2}\times\sqrt{2}$ reconstruction of the substrate. As demonstrated by the analysis of the photoelectron diffraction patterns, the oxygen atoms sit thereby in a $c(2\times2)$ arrangement in the previous fourfold hollow sites nearly coplanar with the Ag atoms, while rows of substrate atoms are removed along the [100] directions. Annealing the crystal above 350 K restores the $p(1\times1)$ symmetry and the oxygen moves to 0.6 Å above the fourfold hollow site. It becomes then more oxidic in nature, as demonstrated by the shift of the O $1s$ level from 530.3 eV to 528.3 eV. The phase transition affects also the O $2s$ and O $2p$ levels as well as the surface component of Ag $3d_{5/2}$. The vibrational frequency of the oxygen adatoms against the surface decreases at the phase transition, in accord with the larger adsorption distance. The higher temperature phase is active towards CO and C_2H_4 oxidation, while the low-temperature phase is not. When cooling the sample below room temperature the reconstructed phase is restored. The time constant of this process as well as the chemical reactivity of the high-temperature phase are weakly reproducible since they depend on the previous history, i.e., presumably on the subsurface oxygen content of the sample.

I. INTRODUCTION

Oxygen interaction with Ag surfaces attracted much attention over the past years because of the unique role played by Ag powders as an extremely selective catalyst for the ethylene epoxidation reaction,[1,2] which is at the basis of a large industry. Although highly qualified work was performed over the last three decades on the O/Ag and O_2/Ag systems, which are therefore quite well characterized, the reaction could not be reproduced under controlled conditions and the nature of the active oxygen has so far escaped understanding. Recently O_2/Ag was taken as a paradigm for the study of the dynamics of the gas-phase interaction with a solid surface.[3]

Most of the investigations dealt with Ag(110) and Ag(111), leaving Ag(001) aside as a less interesting case, which was believed to have intermediate properties between the open and the closed-packed surfaces. Already in the early days, however, Engelhardt and Menzel[4] noticed that, contrary to the other low Miller index surfaces,[5] for O/Ag(001) the work function decreased upon oxygen exposure when the crystal was below room temperature. This behavior is also opposite to the one expected for an electronegative adsorbate and it was suggested to be due to subsurface migration of the oxygen atoms. In spite of the prominent role proposed for subsurface oxygen in the epoxidation reaction,[2] it was not investigated further.

More recently we found, by supersonic molecular beam and high-resolution electron-energy-loss spectroscopy (HREELS) investigation, that O_2 chemisorbed on Ag(001) is indeed very similar to O_2 chemisorbed on Ag(110), as they have nearly the same internal vibrational frequency and potential-energy barrier to adsorption.[6,7] However for the former, system dissociation takes place only at defect sites, which we identified with kinks.[8] For this reason the dissociation probability is very low and at room temperature we found a saturation coverage of 0.1 ML of oxygen adatoms, when dosing with the supersonic molecular beam.[6] In accord with the low coverage value, no low-energy electron diffraction (LEED) superstructures were observed, while the vibrational frequency $\hbar\omega$ read 34 meV. When heating the crystal no recombinative thermal desorption took place, confirming that oxygen is efficiently incorporated into the bulk.

C. S. Ares Fang[9] reported the formation of a weak $c(2\times2)$ phase and $\hbar\omega=37$ meV, when dosing at 180 K, and the formation of a (1×1) phase with $\hbar\omega=30$ meV, when dosing O_2 at room temperature. Even if in our previous experimental investigations we could not reproduce such superstructure,[8] we show in the present paper that it can be formed but only when dosing at crystal temperatures around 150 K. On the other hand, we observed that oxygen adatoms with different vibrational frequencies form upon nonthermally induced dissociation, i.e., either by CO oxidation [$\hbar\omega=35$ meV (Ref. 10)] or by collision with energetic Xe atoms (loss peaks appeared at 28 meV and either at 33 meV or 36 meV, depending on the angle of incidence and impact energy of the Xe atoms.[11]) The energy loss $\hbar\omega$ decreased moreover to 31 meV when heating the crystal above room temperature.[12] Such change was correlated with the disap-

pearance of a further loss at 130 meV, which we assigned to the presence of subsurface oxygen.[12]

Similar high-energy-loss features were reported by Pettinger *et al.*[13] for the other low Miller index surfaces when exposing O_2 at atmospheric pressure. The same group showed with x-ray photoemission spectroscopy (XPS) measurements that, under such conditions, several atomic oxygen moieties form on Ag(111):[14,15] O_α, corresponding to adatoms on nonreconstructed areas, at a binding energy $E_B(O\,1s)$ between 530.4 eV and 530.6 eV; O_β, atoms dissolved into the bulk, at $E_B(O\,1s)$ in the range from 530 eV to 531 eV, depending on abundance; O_γ, surface oxide on reconstructed islands, at 529.0 eV. These species are different from the oxygen adatoms obtained under controlled ultrahigh vacuum (UHV) conditions by Campbell on Ag(110) (Ref. 16) and Ag(111),[17] whose $1s$ binding energy is 528.3 eV.

The presence of more than one atomic oxygen moiety on Ag surfaces after massive O_2 exposures (30 min at 0.1 Pa at a crystal temperature between 570 K and 700 K) was reported also for Ag foils,[18,19] where XPS peaks with binding energies of 528.3 eV (oxidic oxygen) and 530.3 eV (covalent oxygen) were observed. Such oxygen species showed very different chemical reactivity[20] towards C_2H_4. The same moieties were produced also by exposing the crystal to a reaction mixture of O_2 and CO or C_2H_4.[21] Such treatment did not cause a better characterized ''surface modification,'' which seemingly activated the Ag surface with respect to the ethylene epoxidation reaction.[20] Coadsorption of both oxygen moieties was thereby found to be essential for the production of ethylene epoxide.

The presence of a reactive and of an unreactive oxygen species towards CO oxidation was reported for O/Ag(110) (Ref. 22) when preparing the oxygen layer and dosing CO below 200 K in UHV conditions. No spectroscopic investigation was, however, performed for this system.

In order to verify the possible connection of such oxygen species with the ones associated to the different vibrational frequencies observed by HREELS on Ag(001) under controlled conditions, we investigated this system thoroughly by x-ray photoemission spectroscopy, x-ray photoelectron diffraction (XPD), HREELS, and LEED inspection. For the XPS and XPD study we used three beam times at the SuperESCA beam line at the ELETTRA synchrotron in Trieste, while the HREELS study was performed in Genova.

II. EXPERIMENT

The experimental set-up in Genova was described in detail in Ref. 23. It allows us to deposit the O_2 by a supersonic molecular beam and to perform HREELS measurements at crystal temperatures down to 100 K. With the help of the beam a high-sticking coefficient, $S \approx 0.7$, can be reached also for O_2/Ag(001), thus allowing us to reduce the O_2 exposure time and to work in better vacuum conditions.[7] In part of the measurements, however, the oxygen was dosed by backfilling [dissociative sticking coefficient of about 10^{-4} (Refs. 6 and 24)] in order to reproduce the same experimental conditions as for the measurements performed at ELETTRA. The adsorbed species were monitored and identified by HREELS, which was operated at a resolution between 5 and 8 meV.

The XPS experiments were performed at ELETTRA with the SuperESCA beam line, which allows for an intense photon flux (up to 10^{12} photons/sec for photon energies $h\nu$ below 0.7 keV, with a resolving power above 5000). A description of the setup can be found in Ref. 25. The measurements were recorded in several beam times using two different Ag crystals and sample mountings. The manipulator allowed us to change the azimuthal angle of the sample (the angle between photon beam and detector is fixed and reads 40°), while cooling was limited to 120 K. The very intense light beam of ELETTRA allowed us to record the XPS spectra within few minutes, thus allowing to follow the time evolution of the adsorbed species. The photon flux had no influence on the O adatoms while it induced desorption and/or dissociation of the O_2 admolecules.[12]

The estimated relative error in the energy positions of the XPS peaks in our study is ± 0.05 eV. The XPS binding energies E_B were calibrated against the bulk Ag $3d_{5/2}$ peak value of 368.0 eV to be in accord with the principal XPS papers with which we shall compare our data, i.e., Weaver and Hoflund,[26] Bukhtyarov and co-workers,[18,21,20] and Bao and co-workers.[13,15] Citrin *et al.*,[27] and Andersen *et al.*[28] reported, on the other hand, 368.2 eV for the Ag $3d_{5/2}$ peak position.

The photon beam is plane polarized. The polar XPD curves (as the ones reported in Figs. 10 and 11) are therefore not symmetric with respect to the polar angle θ because the polarization of the light changes from nearly normal to the surface at $\theta = -40°$ (grazing incidence of the photon beam) to parallel to it at $\theta = +40°$.

Calibration of the surface coverage, Θ_O, for O/Ag(001) is problematic as no thermal desorption is observed,[12] the oxygen Auger signal on Ag is very small, and only one LEED superstructure corresponding to the low-temperature phase of adatoms, is present. For the experiments in Genova, we estimated the coverage from the intensity of the losses measured by HREELS assuming the dipole moment to be the same as for O/Ag(110), for which calibration with known LEED structures is possible.[29] For the synchrotron data (recorded at ELETTRA) Θ_O was estimated from the O1s peak area, calibrated to the XPS signal of the sharp $c(2\times2)$ LEED pattern of the low-temperature oxygen phase. Such superstructure corresponds to a nominal coverage of 0.5 ML, but, as discussed later (Sec. III C), it is in reality a disordered $2\sqrt{2}\times\sqrt{2}$ phase, whose extra spots are too weak to be visible. The coverage should therefore be smaller than 0.5 ML, but large enough to give rise to an ordered $c(2\times2)$ structure of the oxygen adatoms. A fully developed $2\sqrt{2}\times\sqrt{2}$ structure could not be achieved as, due to the vanishing O_2 sticking coefficient at large coverage, further dosing would have inevitably increased also the contamination level (in particular of C containing species).

As no better evaluation of Θ_O was possible, we assumed $\Theta_O = 0.4$ ML for the $c(2\times2)$ superstructure. This assignment is confirmed by comparing the XPS intensities with the one obtained under identical experimental conditions for the known $c(2\times2)$ O/Rh(001) system, for which $\Theta_O = 0.5$ ML. Since no direct calibration is possible for the high-temperature O moiety, we used for it the same calibration as for the low-temperature phase. This choice for the measurement conditions at $h\nu = 655$ eV, $\phi = 20°$, and $\theta =$
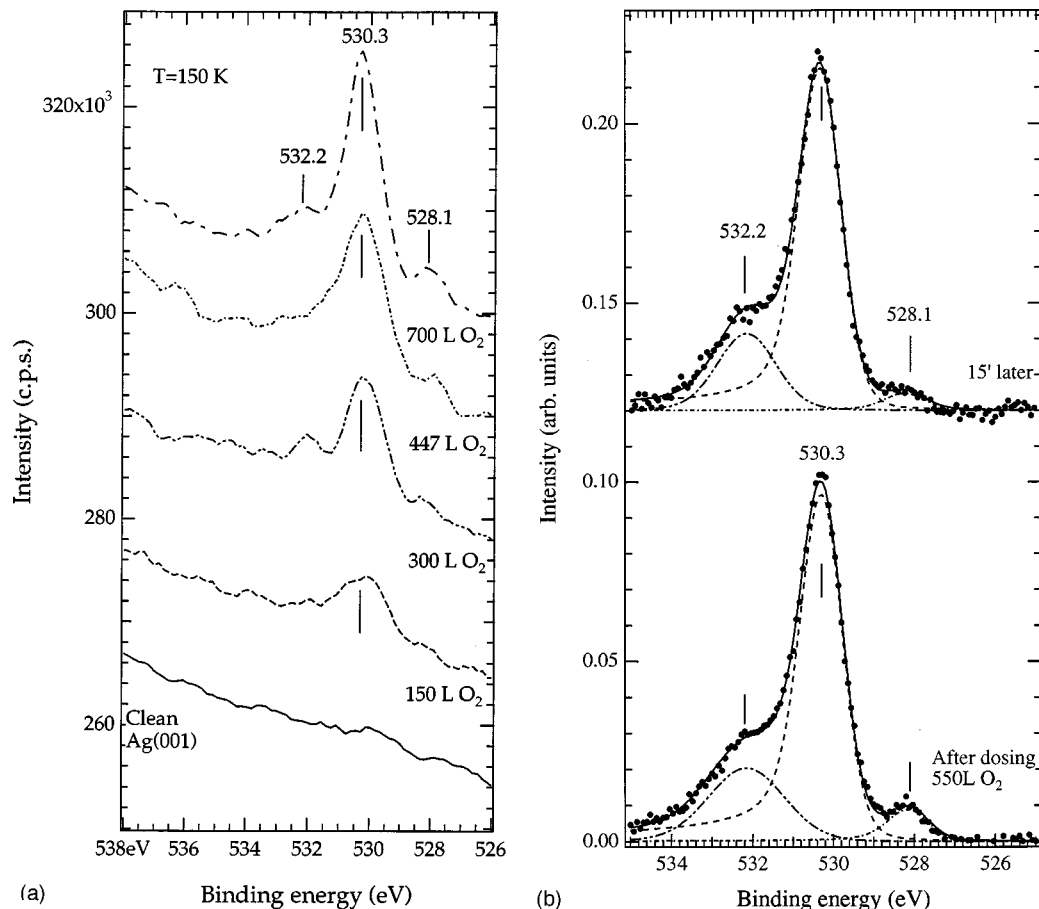
FIG. 1. (a) XPS spectra recorded vs oxygen exposure at $T=150$ K. Oxygen peaks form at $E_B(O\,1s)=532.2$ eV, 530.3 eV, and 528.1 eV. The last moiety is unstable at this temperature as demonstrated in (b). Contamination with carbon containing species is negligible. The spectra in this and in the following figures were normalized to the background and are rigidly shifted except for the bottom curve. The O $1s$ spectra were recorded at $h\nu=655$ eV, $\theta=-40°$, and $\phi=21°$ off $\langle 100 \rangle$.

$-40°$ is justified *a posteriori* from the analysis of the photoelectron diffraction (see Sec. III C).

III. DATA PRESENTATION

A. Experiments at SuperESCA

1. XPS

(a) *Oxygen uptake.* Typical XPS spectra recorded sequentially while dosing O_2 at T=150 K are reported in Fig. 1(a). The spectra were recorded at a photon energy $h\nu$ of 655 eV, corresponding to a photoelectron kinetic energy of 125 eV, to enhance surface sensitivity. A major peak, growing with oxygen dosis, is observed at a binding energy $E_B(O\,1s)$ of 530.3 eV. This value coincides with the one of the "covalent" oxygen of Bukthyarov *et al.*[18,20] and Boronin *et al.*[19] and of the O_α and O_β species reported by Bao and co-workers.[13,15] To our knowledge, this is the first time that oxygen with $E_B(O1s)=530.3$ eV is produced under controlled conditions. This binding energy would also be appropriate for carbonates [$E_B(O\,1s)=529.9$ eV,[16]] but we can safely exclude contamination with carbon containing species by inspection of the C 1s region. The control was performed at $h\nu=432$ eV, corresponding to a sensitivity comparable to the one that we have for oxygen at $h\nu=655$ eV.

Minor peaks are present at 532.2 eV and 528.1 eV. The former corresponds to adsorbed O_2; the latter is due to another oxygen moiety that is unstable at this temperature and disappears with time [Fig. 1(b)]. Its binding energy coincides with the one of the adatoms obtained by thermal dissociation of O_2 on Ag(110) and Ag(111).[16,17]

The area of the main peak in Fig. 1(a) was evaluated with a fitting algorithm based on the Doniac-Sunjic form. In Fig. 2 we report this quantity vs O_2 exposure for uptakes recorded at different T. The slope of the curves is proportional to the dissociative sticking coefficient S, which is estimated to be 7.4 10^{-4} at $T=150$ K and 1.3 10^{-4} at $T=250$ K and was even smaller above room temperature. The value at 250 K compares well with our previous molecular beam study of S.[6] This behavior is at variance with our results obtained with the supersonic beam, where we found an increase of S with T above 180 K (Ref. 8) connected to the thermally activated generation of kinks. The different behavior of S in the present experiment must be connected to the different impact energy: 800 meV with the beam vs 25 meV in the backfilling experiments.

The dissociation mechanism active at 150 K allows to reach, after a dosis of some 3000 L of O_2, a coverage which is large enough to form a $c(2\times2)$ LEED superstructure. The LEED result of C. S. Ares Fang[9] is thus confirmed except
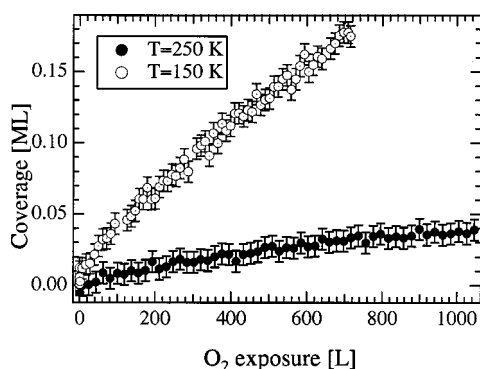
FIG. 2. Atomic oxygen coverage of O530 vs O_2 exposure at two different crystal temperatures. Oxygen is dosed by backfilling and adsorption occurs in both cases dissociatively. 1 L corresponds to a dose of 0.32 ML of O_2 impinging on the surface. The slope of the uptake curves is proportional to the sticking coefficient.

that the dosing temperature must have been lower than 180 K.

At still lower temperatures also nondissociative adsorption takes place, as demonstrated by the presence of the oxygen peak at 532.2 eV. Such peak disappears at 160 K, in accord with the temperature of thermal desorption and dissociation of O_2.[30] Possible contamination with H_2O and OH, which have $O(1s)$ peaks at the same E_B value, can be ruled out because such species have a higher desorption temperature as proved by XPS and HREELS dosing H_2O on purpose. The measured value of $E_B(O 1s)$ falls into the range appropriate to peroxides[31] in accord with the HREELS results.[32] As the vibrational frequencies of $O_2/Ag(001)$ and of $O_2/Ag(110)$ are very similar, the chemisorption sites should be similar, too. The $E_B(O1s)$ value of 529.3 eV reported by Campbell for the latter system[16] looks therefore anomalously low. The same author reported moreover a binding energy of 531.5 eV for $O_2/Ag(111)$ (Ref. 17) and assigned it to superoxide. According to Qiu *et al.*,[31] however, this moiety should have $E_B(O1s)$ values in the range of 535 eV and can thus be excluded. Most probably, O_2 adsorption occurs therefore in peroxide form also for Ag(111) and the low value reported by C.T. Cambell for $O_2/Ag(110)$ is wrong.

As shown in Fig. 3 the intensity of the peak at 532 eV is heavily affected by the photon beam, which causes dissociation, and probably also desorption, of the admolecules most likely via the production of secondary electrons.[12]

Our XPS experiment indicates that carbonate formation becomes important when dosing O_2 below 140 K. In order to minimize oxygen dosis and C contamination, the oxygen exposure was therefore performed at $T \geq 150$ K for the backfilling experiments discussed in the following.

(b) *Phase transition.* When heating the crystal, the oxygen species with $E_B(O 1s) = 530.3$ eV is present up to $T = 300$ K. It disappears eventually if the experiment is performed immediately after repeated cleaning cycles or if the initial coverage is low [see Fig. 4(a)]. As no recombinative desorption is observed, we conclude that subsurface migration takes place. On the other hand, if the initial coverage is large, partial conversion into another oxygen moiety, characterized by $E_B(O 1s) = 528.3$ eV, takes place [Fig. 4(b)]. We conclude therefore that the phase conversion of the adatoms
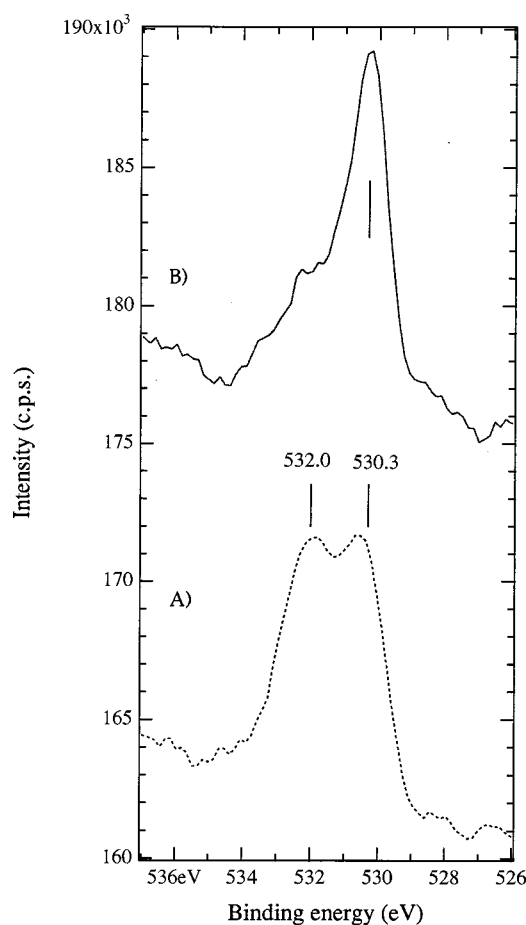

FIG. 3. XPS spectra in the O 1s region after adsorption at $T = 120$ K. Spectrum A corresponds to a virgin spot of the crystal, while spectrum B was recorded after prolonged exposure to the photon beam, which induced O_2 desorption and dissociation of oxygen admolecules [$E_B(O 1s) = 532$ eV].

can occur only if the concentration of oxygen dissolved in the bulk is larger than some critical value. For brevity in the following we will refer to the two atomic oxygen phases as O530 and O528. The oxygen dissolved into the bulk is not visible in our XPS spectra as, at a photoelectron kinetic energy of 120 eV, the information depth is limited to 2–3-Ag layers. It was observed however with conventional x-ray sources by Bao *et al.*[15] (O_β moiety) for heavily oxidized Ag(111) at $E_B(O 1s)$ values ranging from 531 to 530 eV, depending on abundance. In agreement with this we find that after O530 disappearence a small peak is present at $E_B(O 1s) = 530.9$ eV, which we assign to oxygen in subsurface sites (see Fig. 4). Such a peak might have been present also before annealing but becomes visible only after the larger XPS intensity due to O530 is removed. We identify the subsurface oxygen moiety (O531 in the following) with the one responsible for the energy loss at 130 meV observed by HREELS, as both disappear at $T = 350$ K.[12] Contrary to the O_β moiety of Bao *et al.*,[15] its site must therefore be in the immediate subsurface region, i.e., in the first Ag layer, presumably in the octahedral interstitial. O531 is also observed in the initial stages of the backconversion process [see Fig. 6(a)].

The $c(2 \times 2)$ superlattice LEED spots disappear at 300 K, i.e., when conversion into O528 starts. We are therefore
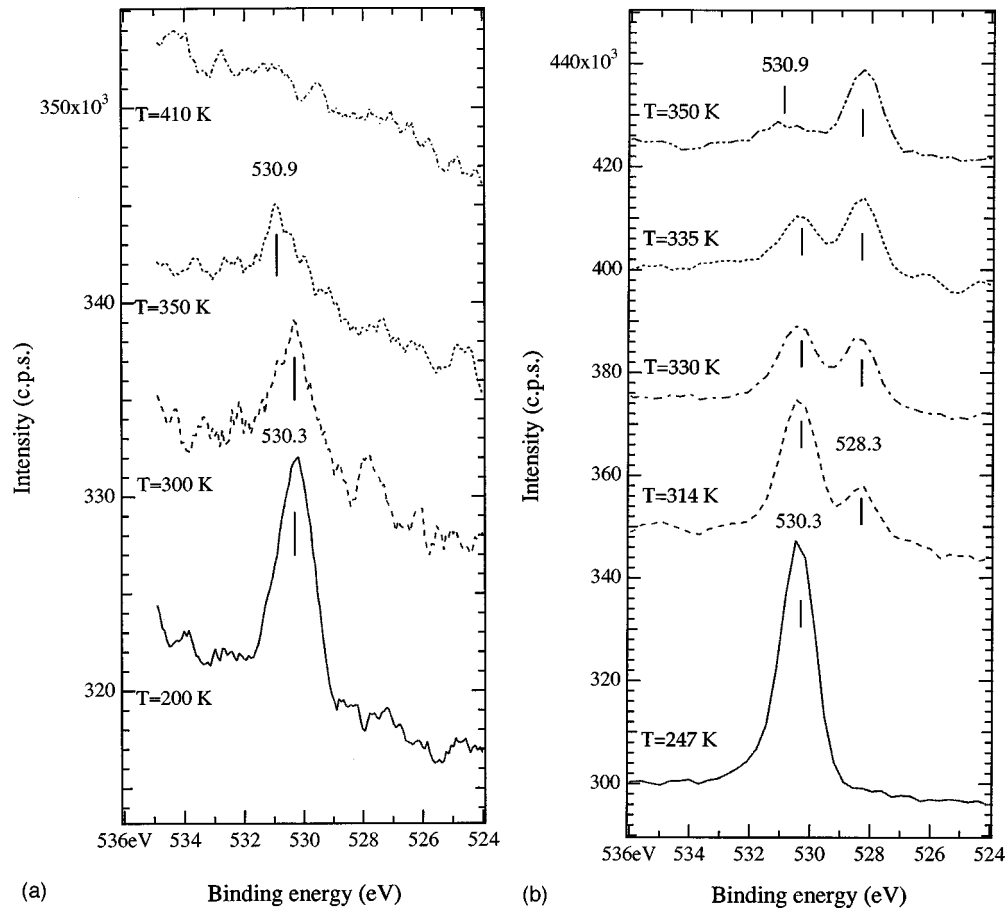
FIG. 4. Evolution of the XPS spectra vs annealing temperature for (a) low coverage ($\Theta_O = 0.05$ ML) and (b) high coverage ($\Theta_O = 0.22$ ML). At $T = 300$ K the oxygen starts converting from the phase with a binding energy of 530.3 eV (O530) to the one with a binding energy of 528.3 eV (O528) only if the initial O530 coverage and the subsurface oxygen content are large enough. Prior to disappearing the oxygen $1s$ peak shifts to 530.9 eV (O531).

dealing with a phase transition as the formation of the high-temperature phase is associated with a reduction of the surface symmetry. As we will demonstrate below the $c(2 \times 2)$ superstructure corresponds in reality to a $2\sqrt{2} \times \sqrt{2}$ reconstruction of the substrate, whereby the quarter order spots are too weak to be observed by visual inspection of the LEED screen. A similar structure forms for O/Cu(001) (Refs. 33–35) and also in that case the quarter order spots are hardly visible at low coverage.[33,34] Interestingly, O/Cu(001) also has a binding energy of 530 eV.[36,37]

The intensity of the oxygen moieties shown in Fig. 4(b) is reported in Fig. 5 vs T. As, for the present experimental conditions ($h\nu = 655$ eV, $\theta = 40°$), the photoemission cross sections of O530 and O528 are both close to their average value (see XPD data in Sec. III C) the peak areas allow to directly estimate the relative surface coverage. Inspection of the figure shows therefore that while heating the crystal above the transition temperature roughly half of the oxygen dissolves into the bulk. Subsurface diffusion was reported also for O/Ag(110) by C. Backx et al.,[5] but in that case the dissolution temperature was above 450 K.

O528 converts back to O530 when cooling below room temperature and, if the final coverage is large enough, the $c(2 \times 2)$ LEED pattern is restored. As shown in the first spectra of Fig. 6(a), $E_B(O\,1s)$ has initially a value of 530.7 eV and then shifts to 530.3 eV. Such shift is indicative of

oxygen segregation from the bulk; direct conversion of O528 into O530 becomes dominant only eventually. After the backconversion process is completed, O$1s$ binding energy and XPD pattern (see Sec. III C), are identical to the ones of the O530 phase produced by direct dissociation. Adsorption
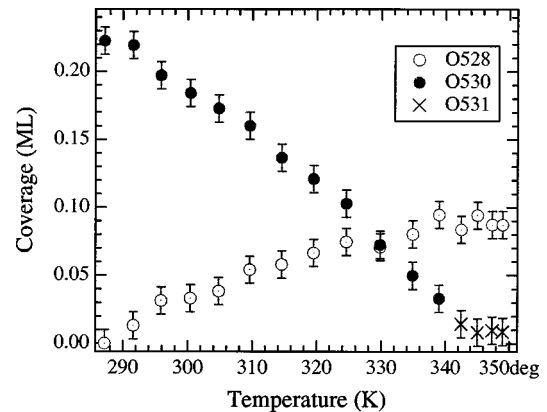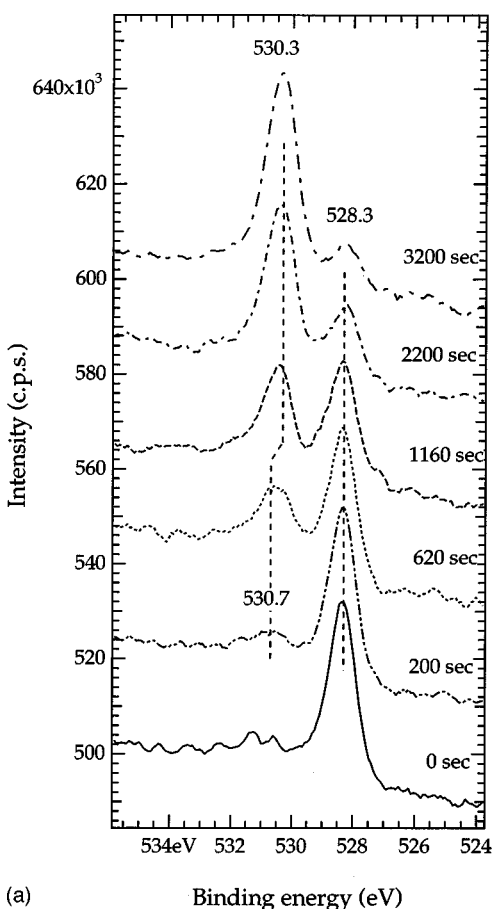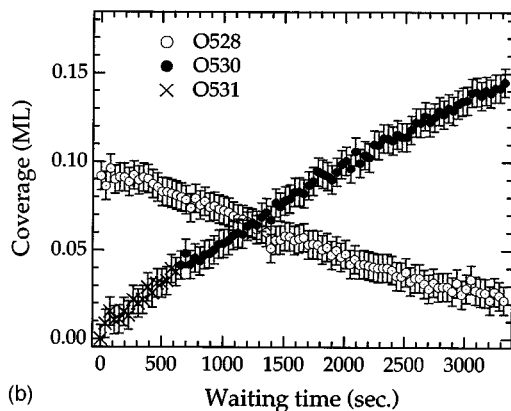

FIG. 5. Oxygen coverage vs T when heating the crystal above the transition temperature for the conditions of Fig. 4(b). The heating rate is 0.4 K/sec. Filled circles and open circles indicate O530 and O528, respectively. Crosses indicate oxygen with a binding energy of 530.9 eV (O531) associated with oxygen occupying sites in the immediate subsurface region.

FIG. 6. (a) Sequence of XPS spectra showing the backconversion process of O528 to O530 when the crystal is cooled to 246 K. The time constant of the process depends on the past history of the sample. It was shorter for a sample that had been exposed to air for several months for which the subsurface oxygen concentration is greater. The spectra were recorded at $\theta=40°$ and $\phi=21°$ off $\langle 100 \rangle$ with $h\nu=655$ eV. (b) Coverages of the three oxygen moieties vs time. Note the delayed onset of the depletion of O528 after cooling the sample.

site and chemical state of the O530 adatoms are therefore the same before and after conversion into O528.

The O528 and O530 coverages, recorded during the backconversion process, are reported in Fig. 6(b). As one can see, the removal of O528 starts only after ≈ 500 sec, during which oxygen segregation to the immediate subsurface region (O531 moiety) occurs. Because of this effect the appar-
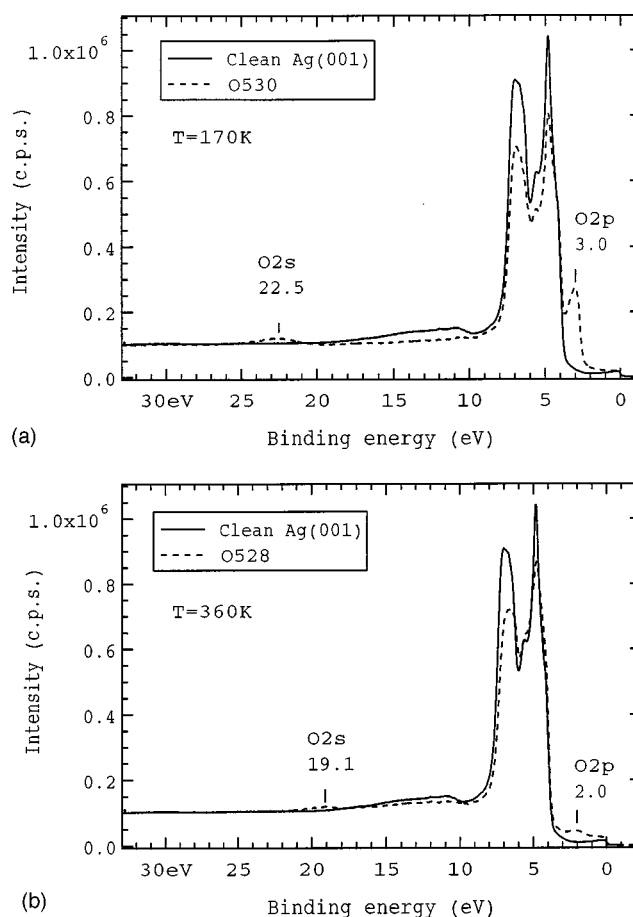

FIG. 7. Valence bands of the clean Ag surface (continuous line) and after adsorption of the two oxygen moieties (dashed line) at given crystal temperature: (a) O530, (b) O528. The position of the O 2s and O 2p levels is show by the bars. The spectra were recorded at $\theta=37°$ and $\phi=0$ ($\langle 100 \rangle$ direction) with $h\nu=182$ eV.

ent final coverage of O530 is slightly larger than the initial coverage of O528. The time constants of O530 formation and O528 removal processes were not reproducible between the different experimental runs and were sometimes quite different between each other. The irreproducibility indicates that the backconversion process is determined not only by crystal temperature, but also by the previous history of the sample, i.e., presumably by the dissolved oxygen concentration. The difference between the time constants of O528 and O530 confirms that segregation from the bulk contributes significantly to the O530 signal. The measured time constant for O528 disappearence ranged between 3000 and 20000 sec.

Since the backconversion process took place also at 140 K the energy barriers to be overcome must be small.

2. Valence-band region

The spectra of the valence band region in presence of O530 and O528 are shown in Figs. 7(a) and 7(b). They were recorded with $h\nu=182$ eV to enhance surface sensitivity. Given the emission angle of 37° the momentum parallel to the surface is 0.9 Å^{-1} along $\bar{\Gamma}$-$\bar{M}$ in the second Brillouin zone. A spectrum of the clean surface recorded in identical conditions is reported for comparison (solid lines). In presence of O530, extra intensity forms at 22.5 eV and 3.0 eV
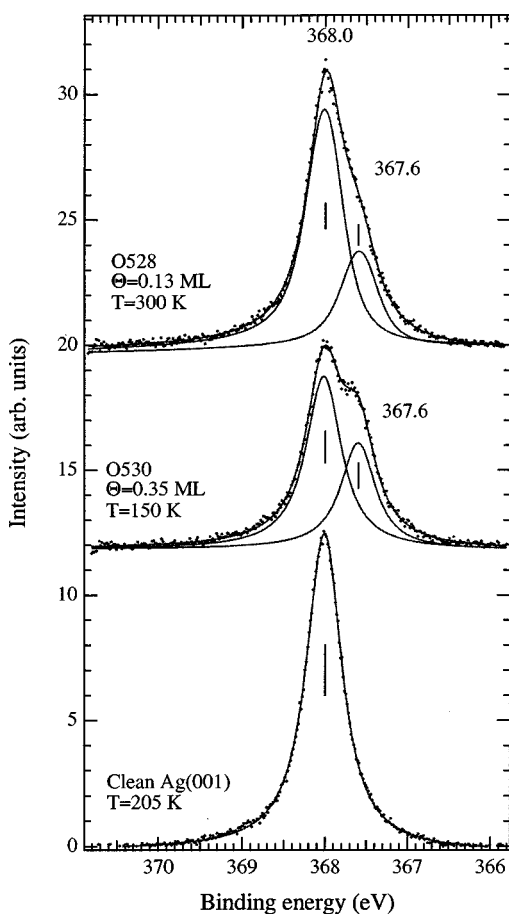
FIG. 8. Ag $3d_{5/2}$ peak for the clean surface, and in presence of O530 and O528. In both cases a core-level shift of -0.4 eV is evident for the Ag atoms in contact with the oxygen. The clean surface core-level shift is negligeable in accord with literature (Ref. 27). The spectra were recorded at $\theta=37°$ and $\phi=21°$ off $\langle 100\rangle$ with $h\nu=471$ eV.

below the Fermi edge, due, respectively, to electron emission from the O $2s$ and O $2p$ orbitals. The intensity between 10 and 15 eV below E_F is due to plasmon excitation, which is heavily reduced in presence of oxygen.[38] For O528 [Fig. 6(b)] the O $2s$ and O $2p$ peaks shift to 19.1 eV and 2.0 eV below E_F, respectively.

The O $2p$ values compare well with those reported for Ag(110), where a dispersion from -3.3 eV at $\bar{\Gamma}$ to -1.5 eV at $\bar{Y}$ (Ref. 39) was observed, and for Ag(111) where the O $2p$ level is at -2.0 eV.[40]

We notice that no extra features are present in the valence band confirming the low contamination level in the reported experiments. In particular, no peaks are observed in the range 11–13 eV below E_F where we would expect the $1\pi_u$, $3\sigma_g$, and $4\sigma_g$ states of CO_2^-, nor at 8.4 eV where CO_3^- has its $3e'$ and $1a_2''$ levels.[14]

3. Ag $3d_{5/2}$

Oxygen adsorption affects also the surface core-level shift of Ag $3d_{5/2}$ as shown in Fig. 8. In accordance with literature,[27,28] bulk and surface components cannot be resolved for the clean surface as they are separated by only 72 meV for polycrystalline Ag. On the other hand, two peaks

are visible after oxygen exposure: one at 368.0 eV due to bulk Ag, and another at 367.6 eV due to Ag atoms in contact with oxygen. The surface component of the O530 phase is only slightly larger than the bulk one. For O528, on the contrary, it is significantly broader because of the larger surface disorder.

The observed binding-energy shift (-0.4 eV) is close to the value of -0.3 eV, reported in literature for Ag_2O.[26] It has an opposite sign than expected between a metal and its oxides[41] and it must therefore be governed by factors others than the electronegativity, such as lattice potential and extra atomic relaxation energy. Other examples of negative shifts were reported for Cd compounds.[41] The anomalous sign is considered indicative of the formation of Ag^+ ions.

As for AgO, the core-level shift reads -0.7 eV,[26] we can conclude that the surface compounds formed on Ag(001) must bear more similarity to Ag_2O than to AgO for both oxygen phases.

B. HREELS investigation

HREEL spectra obtained after dosing O_2 with the supersonic molecular beam at 130 K and annealing at different crystal temperatures are reported in Fig. 9. The exposure temperature is slightly lower than the one used for the experiments at ELETTRA as carbonate contamination is negligible when working with the beam. HREEL spectra obtained after dosing by backfilling evidenced a stronger contamination level, especially of OH as demonstrated by a weak loss at $\hbar\omega=445$ meV. The evolution of these spectra after annealing is, however, similar to those obtained after molecular-beam dosing.

The loss peak at 80 meV in the bottom spectrum of Fig. 9 corresponds to the internal O_2 vibration,[32] and is therefore indicative of nondissociative adsorption. The loss at 30 meV was previously assigned to the O_2 vibration against the surface.[6,7] In the present case, however, it is much more intense than when adsorbing at $T=100$ K and, as demonstrated by the second spectrum from the bottom, its intensity is not proportional to the one of the O_2 peak. It must therefore be due to atomic oxygen, demonstrating that a thermal dissociation channel opens already at $T=130$ K.[42] This kind of oxygen must be of the O530 moiety as the latter dominates the XPS spectra recorded in identical conditions. The frequency reads 32 meV at 150 K upon oxygen dissociation. When annealing to 190 K a sharp $c(2\times2)$ LEED pattern appears and the frequency shifts to 36 meV.

Above room temperature the LEED pattern reverts to (1 $\times$1) and the vibrational frequency moves back to 28–31 meV, the shift being larger when the initial O530 coverage is greater. From XPS we know that only O528 is present in such conditions.

We remark that the $c(2\times2)$ phase and the 36-meV loss cannot be produced when exposing with the molecular beam at $T=100$ K and then dissociating by heating to 200 K because with this procedure the O_2 population is rapidly brought to temperatures at which desorption is far more efficient than dissociation.[8] The maximum atomic oxygen coverage obtainable remains therefore small. Also in the latter
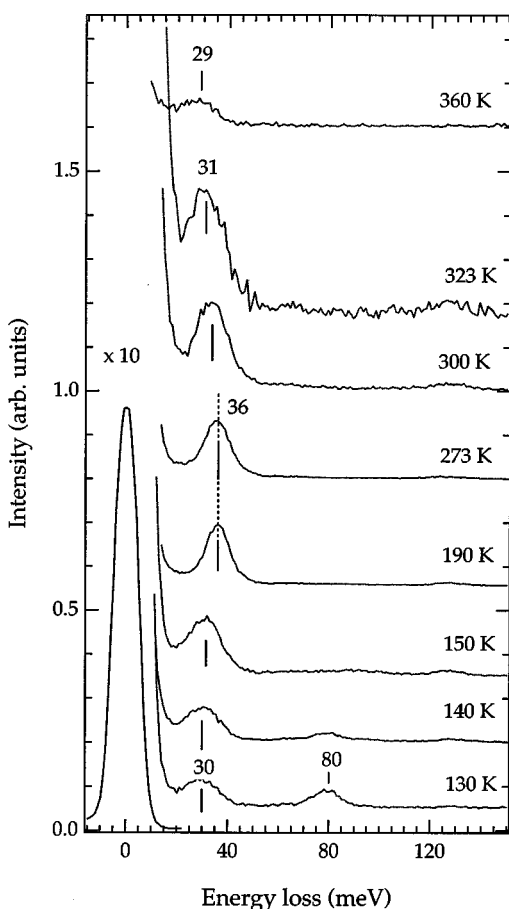
FIG. 9. HREELS spectra recorded after dosing at $T = 130$ K and annealing to different crystal temperatures. The peak at 80 meV is indicative of O_2 adsorption. The peak in the region of 30 meV is due both to molecular oxygen and to oxygen adatoms at low temperature, while it is due solely to adatoms above the desorption temperature of O_2 (150 K, as demonstrated by the disappearence of the peak at 80 meV).

conditions however, a change in the vibrational frequency from 34 meV to 31 meV takes place when heating above room temperature.

C. Photoelectron diffraction

In order to determine the adsorption site and the local surface geometry we recorded the XPS intensity vs azimuthal and polar angle of the sample at $h\nu$ of 655 eV, 710 eV, and 940 eV, corresponding to photoelectron kinetic energies of 120 eV, 175 eV, and 405 eV. The highest-energy data were used to discriminate between different structural models, since they are dominated by forward scattering and allow us to view the atomic structure of the surface in a quasidirect way. At lower kinetic energy on the contrary backscattering becomes important and a full multiple-scattering analysis is necessary.[43]

The polar XPD curves recorded at low energies are reported in Fig. 10 and Fig. 11 for O530 and O528, respectively. Already by visual inspection one can notice that: (a) near normal emission, O530 shows a strong modulation of the intensity at both $h\nu$ values, while (b) the XPD curves for O528 are smoother. This indicates that the adsorption site for
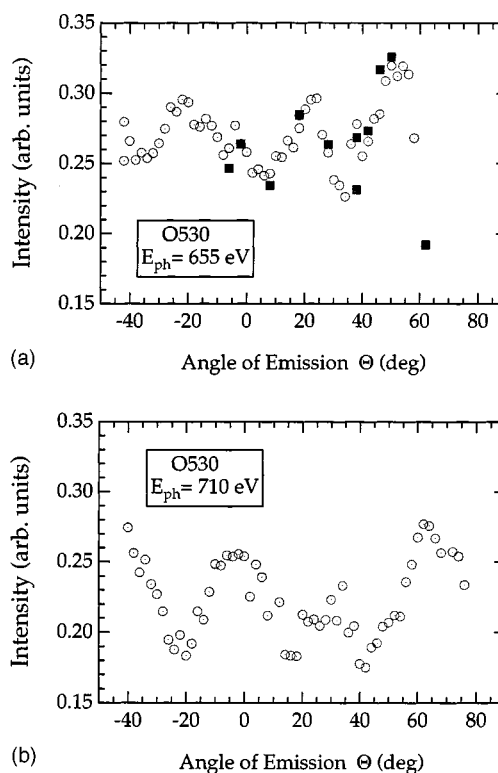

FIG. 10. Polar XPD patterns for O530 for (a) $h\nu = 655$ eV and (b) $h\nu = 710$ eV along $\langle 110 \rangle$. Different symbols indicate different series of measurements. In (a) the □ data were obtained for an oxygen overlayer annealed to 370 K and reconverted to O530 after cooling the crystal below room temperature. The ○ data correspond to an oxygen layer produced by dissociation from the gas phase. As one can see, the XPD patterns are identical within the error.

the two species is different. Such a result is confirmed by the azimuthal scans (see Fig. 12) recorded for both oxygen moieties at the same photon energy ($h\nu = 655$ eV) and polar angle ($\theta = -40°$).

We notice that the photoemission intensity at $h\nu = 655$ eV, $\theta = -40°$, and $\phi = 25°$, i.e., for the conditions at which the spectra shown in Fig. 4 and in Fig. 6(a) were recorded, is close to the average value for both oxygen moieties. This observation justifies *a posteriori* our choice of assuming the same conversion factor for the peak area of O528 and O530 into coverage.

The azimuthal XPD patterns for O530 recorded at $h\nu = 940$ eV are shown in Fig. 13 together with the best fits obtained for different models [all compatible with a $c(2 \times 2)$ LEED pattern at low coverages] with a simulation code based on single-scattering processes.[44] The different investigated models are:

(a) missing-row reconstruction along [100] with a $2\sqrt{2} \times \sqrt{2}$ (rotated 45°) symmetry;

(b) fourfold hollow site with the oxygen sitting slightly subsurface;

(c) oxygen in the octahedral site in the second Ag plane;

(d) oxygen in the tetrahedral site between the first and second plane of Ag;

(e) substitutional oxygen slightly below the first Ag plane.

The best agreement, determined on the basis of an R-factor evaluation,[45] is found for model (a) i.e., for a missing-row reconstructed $2\sqrt{2} \times \sqrt{2}$ structure: oxygen at-
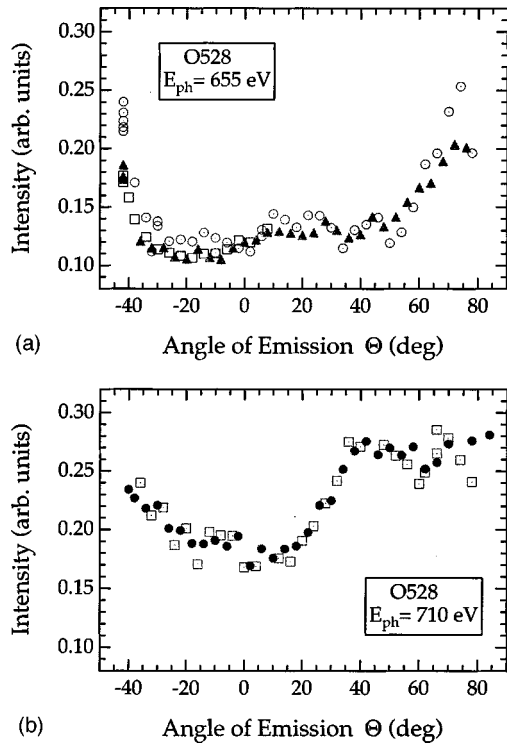
FIG. 11. Same as Fig. 10 for O528: (a) $h\nu = 655$ eV and (b) $h\nu = 710$ eV along $\langle 110 \rangle$. Different symbols indicate different series of measurements.

oms are placed in the missing rows slightly displaced off the previous fourfold hollow sites and slightly subsurface, while also the Ag atoms are relaxed. This structure is similar to the one reported for O/Cu(001) with $\Theta = 0.5$ ML.[34,35] Also in that case the quarter-order spots are extremely faint compared to the half-order ones so that at low coverage a $c(2 \times 2)$ pattern is observed by LEED inspection.

The missing-row reconstructed structure around O530 was investigated by means of low-energy photoelectron diffraction, too. Working in these conditions implies a less straightforward interpretation of the data as backscattering cannot be neglected anymore. On the other hand, the larger photon flux at the SuperESCA beam line allows for a higher quality of the experimental data while the isotropic wave
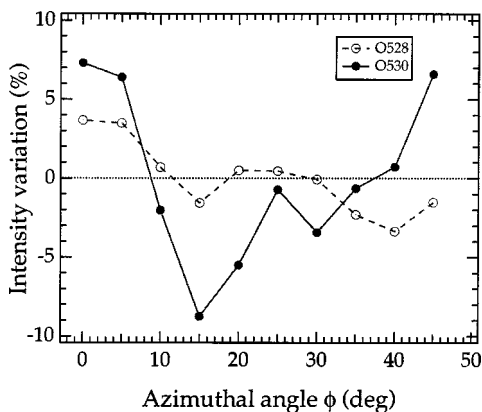

FIG. 12. Comparison of the azimuthal XPD pattern for O530 and O528 at $\theta = -40°$ and $h\nu = 655$ eV. The different modulation is indicative that the two oxygen moieties sit in different sites.
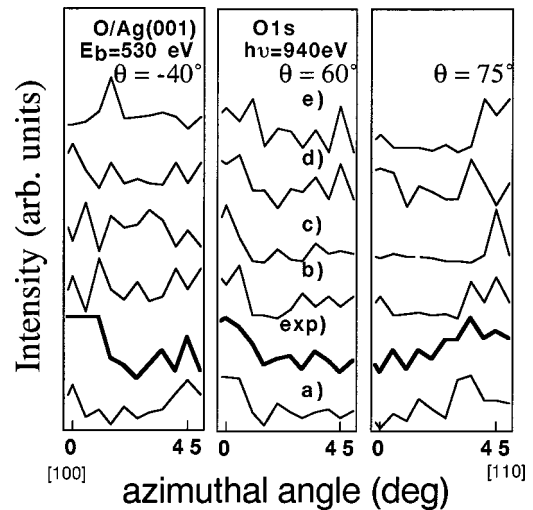

FIG. 13. Comparison of the measured azimuthal XPD patterns of O530 recorded at $h\nu = 940$ eV at different polar angles with the theoretical prediction for different structural models: (a) missing-row reconstruction; (b) fourfold hollow site; (c) octahedral interstitial; (d) tetrahedral insterstitial; (e) substitutional. The best fit is clearly for the missing-row reconstructed surface.

front of the photoemitted electrons is capable of probing the structure with the same accuracy over the whole three-dimensional space. The multiple-scattering modulation was calculated at any order with a self-developed code.[46] A complex exchange and correlation potential allows us to account for the inelastic losses also in the electron path towards the detector. The comparison of the best fit with the experimental data is reported in Fig. 14, while the best-fit structure is shown in Fig. 15. The results confirm that the oxygen atoms are in the previous fourfold hollows displaced towards the missing rows by 0.36 ± 0.04 Å. The adsorption site is 0.15 Å above the outermost Ag plane of the unreconstructed surface. The Ag atoms close to the missing rows are, however, displaced upwards by 0.30 Å and laterally towards the missing rows by less than 0.06 Å, so that the oxygen lies effectively below its nearest Ag neighbors. The main difference with respect to the O/Cu(001) system is that for the latter case the oxygen atoms are displaced away from, instead of towards the missing rows. The different geometry for Ag(001) might be connected to the presence of subsurface oxygen in octahedral sites.

The weakness in the LEED pattern of the quarter-order spots compared to the half-order ones was attributed, in the case of O/Cu(001), to the presence of a well-ordered $c(2 \times 2)$ mesh associated to the oxygen adatoms that are displaced by less than 0.05 Å off the former fourfold hollows.[37] The oxygen layer contributes to the half-order spots, while the disorderly reconstructed substrate determines those of quarter order. There are indeed two different possibilities and two equivalent [100] directions for removing atom rows. This explanation does not hold for O/Ag(001) as the lateral displacement of the oxygen off the former fourfold hollows is large and the scattering strength of Ag is much greater than the one of oxygen. The intensity of the quarter-order spots could, however, be depressed if the missing Ag atoms form antiphase domains shifted by one unit vector of the Ag fcc lattice constant along [001]
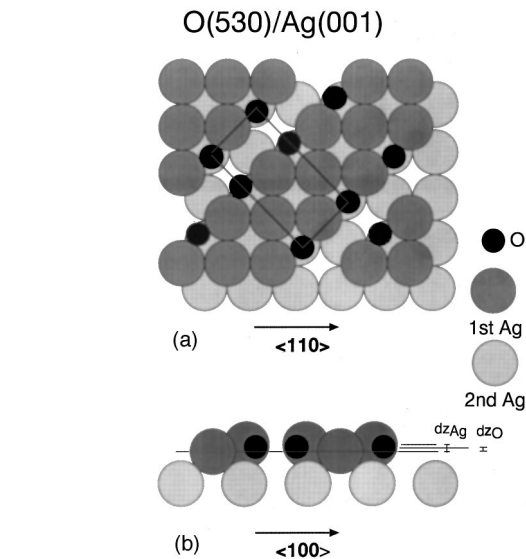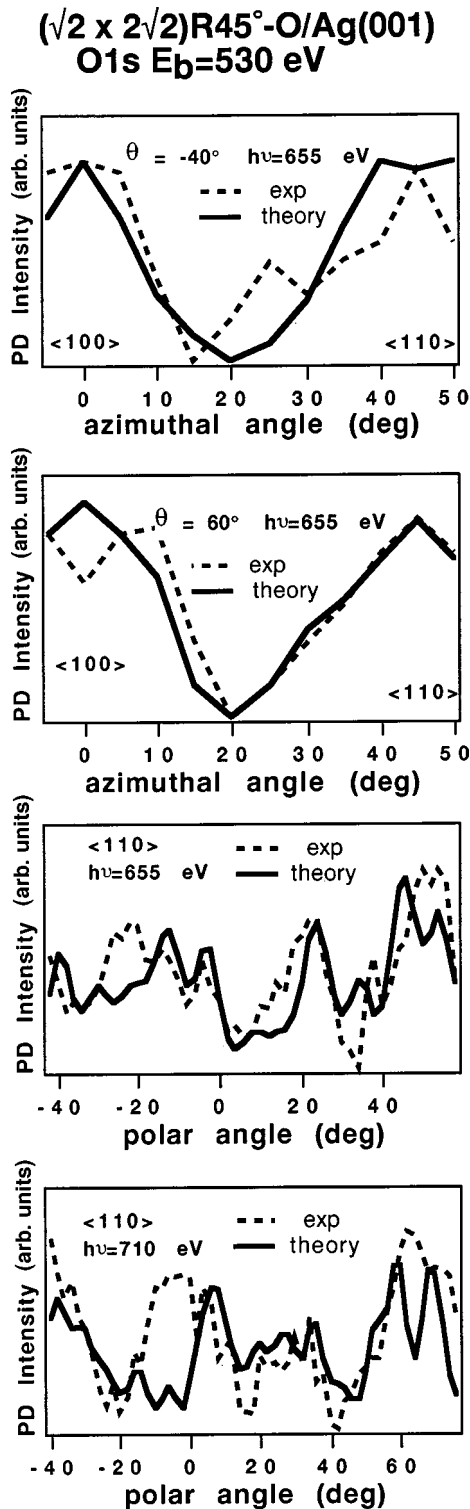
(√2 x 2√2)R45°-O/Ag(001)
O1s E_b=530 eV

FIG. 14. Comparison of the experimental XPD data with the best-fit curves obtained for the $2\sqrt{2}\times\sqrt{2}$ missing-row reconstructed surface.

O(530)/Ag(001)

FIG. 15. Best-fit model for the reconstructed $2\sqrt{2}\times\sqrt{2}$ surface. $d_{z_{Ag}}$ is the height of the surface Ag atoms at the missing rows, with respect to the expected position for an unrelaxed crystal. d_{z_O} is the oxygen-adsorption height with respect to the same reference plane. Contrary to the similar model accepted for O/Cu(001), the O adsorption site is shifted towards the missing rows.

identified with the moiety giving rize to the small peak at $E_B(O\,1s)=528.1$ eV, observed during the oxygen uptake at 150 K.

The presence of some features in the measured XPD curves, which are not completely reproduced by the model, is still matter of investigation. We can exclude them to be due to the presence of subsurface missing rows, as this model gives a worse level of agreement. Most probably they are caused by the presence of intensity associated with O531 (subsurface oxygen).

For O528 the comparison of the data with the simple hollow site gives a good agreement, while models involving substitutional adsorption and reconstructed substrates are unacceptable. The assignment is therefore much more straightforward than in the O530 case. Comparison with experiment for different adsorption heights is reported in Fig. 16(a) for the azimuthal scans at a polar angle of $-40°$ and $h\nu = 655$ eV, and in Figs. 16(b) and 16(c) for polar scans along the [110] direction at $h\nu=655$ eV and $h\nu=710$ eV, respectively. As the experimental areas were normalized to the background, we corrected them by multiplying with cos θ.[47] The best agreement is obtained when the oxygen sits 0.6 Å above the fourfold hollow site of an unreconstructed surface. The sensitivity of photoelectron diffraction to the adsorption height of oxygen is very high in all cases.

D. CO oxidation and chemical reactivity

In a previous investigation we had found the unexpected result that oxygen adatoms on Ag(001) could not be removed by CO oxidation,[10] contrary to the case of the other low Miller index Ag surfaces.[22] Such an experiment was performed below and at room temperature, i.e., for conditions corresponding to the presence of O530. As shown by XPS in Fig. 17, such moiety is indeed chemically inert. O528 on the

(4.06 Å) within the transfer width of our LEED system (typically 100 Å). Constructive interference would then take place for the half-order spots and destructive interference for the quarter-order spots. The position of the missing Ag atoms is most probably dictated by a $c(2\times2)$ mesh of oxygen forming locally prior to the reconstruction. Oxygen sitting in such mesh on a still unreconstructed surface is possibly to be
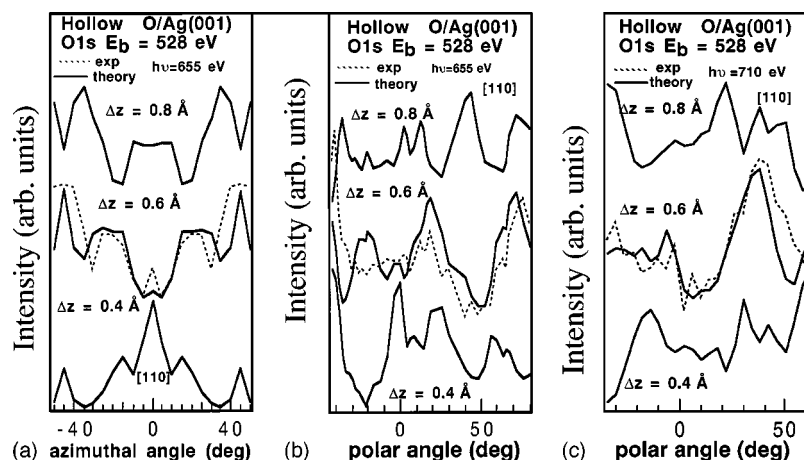
FIG. 16. Comparison of the measured XPD pattern in presence of O528 with the theoretical prediction for the fourfold hollow site at different chemisorption heights: (a) azimuthal curves, (b) and (c) polar curves at different $h\nu$. The areas of the oxygen peaks in b and c were multiplied by $\cos\theta$ in order to compensate for the angle dependence of the background to which the experimental spectra were normalized.

contrary can be readily removed, (see Fig. 18). Similar results were obtained by HREELS investigation and molecular-beam dosing. Interestingly, the XPS spectra show that after the CO reaction with O528 a new peak forms at 529.0 eV, which coincides with a surface oxide moiety observed by X. Bao et al.[13] after extremely large oxygen exposures on Ag(111). This moiety is not removed by further exposure to CO.

The inertness of oxygen in our previous study was thus connected to its O530 nature. Notably, oxygen with similar binding energy was found to be chemically inert also by Bukthyarov et al.[20] and by Felter et al.[40]. The measured reactivity of O528 on Ag(001) is however still one order of magnitude smaller than for O/Ag(110),[22] which is characterized by the similar binding energy of 528.2 eV.[16] The O528
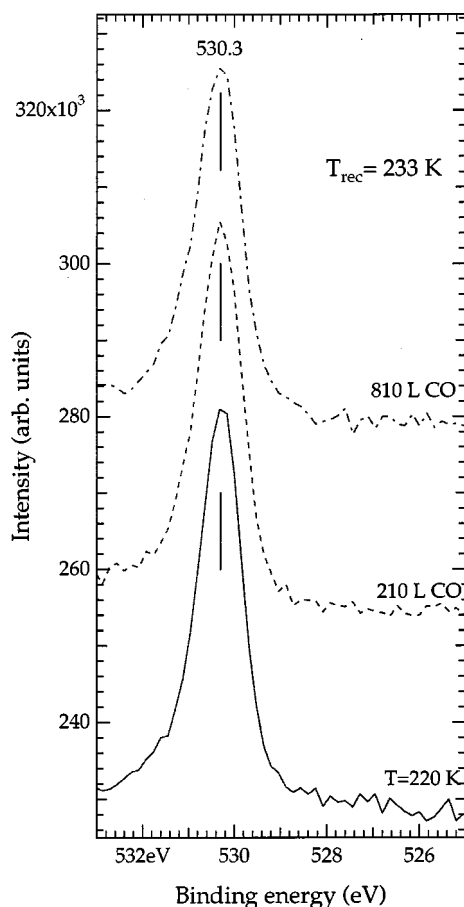

FIG. 17. CO oxidation experiment for O530. No significant reduction of O530 takes place within experimental error, indicating its inertness.
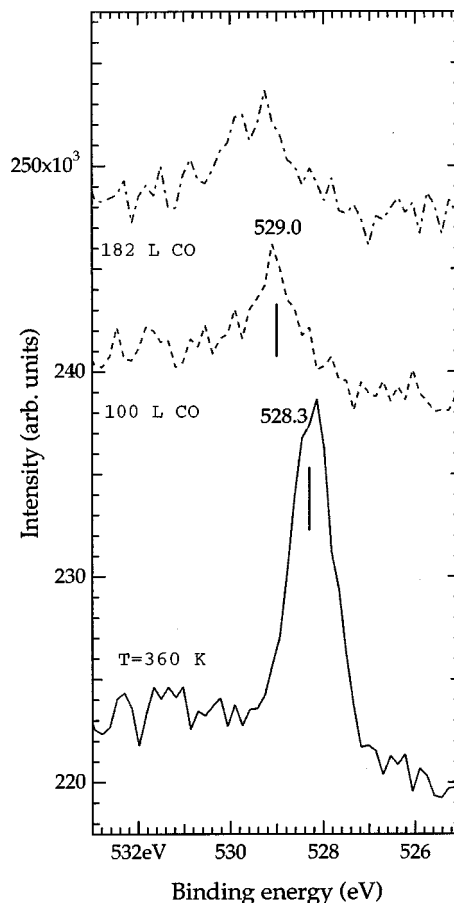

FIG. 18. Removal of O528 by CO exposure. The residual peak at 529 eV has an $E_B(\text{O}\,1s)$ value appropriate to Ag$_2$O (Ref. 26). Rehren et al. associated, however, oxygen with this binding energy on Ag(111) to a particular surface oxygen phase, O_γ (Ref. 14).
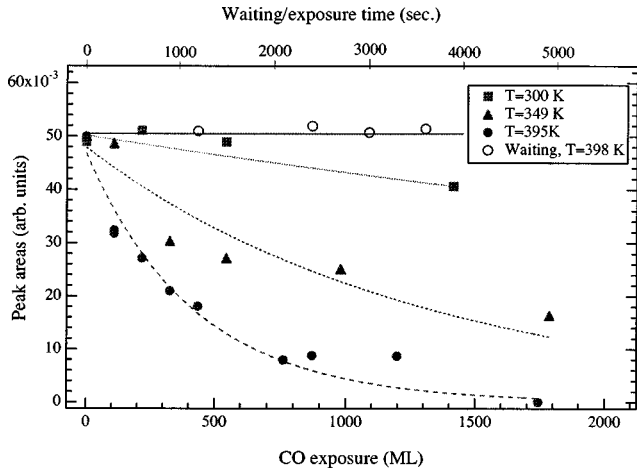
FIG. 19. Intensity of the HREELS oxygen signal vs CO exposure at different crystal temperatures. The corresponding blank experiment is also reported for the high-temperature case: no oxygen removal takes place in the time of the experiment because of subsurface diffusion.

reactivity towards CO came out moreover to be different in the different beam times at ELETTRA indicating its dependence on the previous history of the sample. Indeed it was larger for a run in which the crystal had been exposed to air for several months, and smaller for a run in which the same crystal had been transferred directly from one vacuum chamber to the other. The latter reactivity is consistent with the one found for HREELS measurements performed in Genova on a crystal that had remained in UHV for months. We conclude therefore that the reactivity is dictated by the subsurface concentration of oxygen.

The HREELS results at different crystal temperatures are shown in Fig. 19 together with a waiting experiment. Data recorded below room temperature are not shown since no significant removal occurred. The initial reaction rate, defined by

$$R = \frac{1}{\Theta_O \Phi_{CO}} \frac{\Delta \Theta_O}{\Delta t} (\text{ML}^{-1}), \qquad (1)$$

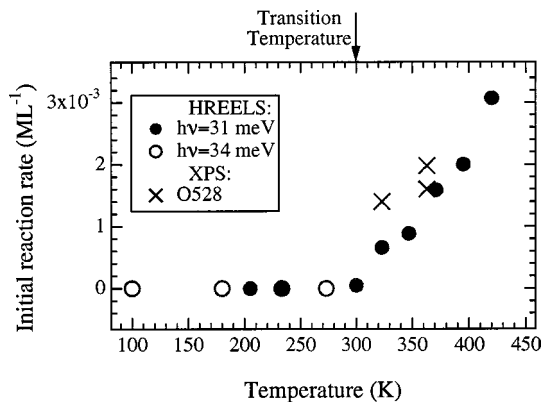where Φ_{CO} denotes the CO flux, is reported in Fig. 20 vs T

FIG. 20. Reactivity of adsorbed oxygen with respect to CO oxidation vs T as inferred from HREELS data. Oxygen vibrating at $\hbar\omega = 34$ meV corresponds to O530, the one at $\hbar\omega = 31$ meV to O528.

TABLE I. O $1s$ binding energies for adsorbed oxygen. When no reference is given, the quoted value was measured in the present experiment. The data of Ref. 48 were recorded for K coadsorption.

Oxygen moiety	Phase	O $1s$ (eV)
O528/Ag(001)	disordered	528.3
O530/Ag(001)	$(2\sqrt{2} \times \sqrt{2})$	530.3
peroxide/Ag(001)	disordered	532.0
O/Ag(110) (Refs. 16 and 51)	p(2×1)	528.1
peroxide/Ag(110) (Ref. 16)		529.3
O/Ag(111) (Ref. 17)	p(4×4)	528.2
O_{ad}/Ag(111) ''active'' (Ref. 40)		528.5
O_{ad}/Ag(111) ''inactive'' (Ref. 40)		530.3
surface oxide on Ag(111) (Ref. 14)		529.0
O_α/Ag(111) (adatoms) (Ref. 14)		530.4
O_β/Ag(111) (subsurface) (Ref. 14)		530.3
O_2/Ag(111) (Ref. 17)		531.5
covalent O/Ag$_{poly}$ (Ref. 19)		530.3
oxidic O/Ag$_{poly}$ (Ref. 19)		528.3
O in bulk (Ref. 14)		531.6–529.7
O/Ag$_{poly}$ weakly bound (Ref. 50)		528.3
O/Ag$_{poly}$ strongly bound (Ref. 50)		530.2
O/Ag$_{poly}$ (low Θ_K) (Ref. 48)		528.5
O/Ag$_{poly}$ (large Θ_K) (Ref. 48)		530.3
O_2/Ag$_{poly}$ (large Θ_K) (Ref. 48)		533.1
O_2/Ag$_{poly}$ peroxide (Ref. 31)		531.5
O_2^{phys} (Ref. 49)		536.5
O_2^{phys} (Ref. 31)		538
Ag$_2$O (Refs. 53 and 41)		529.0
Ag$_2$O (Ref. 26)		528.8
AgO (Ref. 41)		528.3
AgO (Ref. 26)		528.5

and compared with the XPS results obtained in the beam time in which the reactivity was lower. As one can see, the curve is nearly flat up to 300 K in accord with the inertness of O530. On the contrary, as soon as conversion into O528 takes place it starts to increase monotonously. This behavior is indicative of a positive apparent activation energy E_{app}, which results from the subtraction of the desorption energy of CO, E_{des}, from the real activation energy of the oxidation reaction, E_{rea}. A positive value of E_{app} indicates therefore that $E_{rea} > E_{des}$, at variance with the case of CO oxidation of O/Ag(110).[22] This difference is indicative that $E_{des}(Ag(110)) > E_{des}[Ag(001)]$, as indeed expected.

Similar results were obtained for C_2H_4 oxidation. Again O530 resulted to be chemically inert while O528 could be readily removed.

IV. DISCUSSION OF THE RESULTS

The present study is the first in which oxygen atoms with $E_B(O\,1s) = 530.3$ eV are observed on a single-crystal Ag surface under controlled UHV conditions. This oxygen moiety had been previously observed on Ag(111) and on polycrystalline Ag films, as summarized in Table I.

Contrary to our case O530 had then been produced: (i)

either by massive exposures to O_2 at atmospheric pressure[13,14,18] or to reaction mixtures of O_2 and CO or C_2H_4 (Refs. 19–21), (ii) or by coadsorption with alcaline atoms.[48] As conventional laboratory x-rays sources were used in those experiments, carbon contamination could not be checked efficiently. Carbonate formation was, however, excluded in some of these studies because O530 was produced at temperatures at which CO_3^- is unstable.[15] Facetting occurred for the single-crystal experiments of Bao et al.[15]

Bao et al.[13,15] and Rehren et al.[14] found two kinds of O530: O_α corresponding to adatoms and O_β assigned to oxygen dissolved in the bulk. The two species could be distinguished because the latter was not removed by mild sputtering. Bukthyarov et al.[21] assigned O530 to covalent oxygen sitting in supersurface sites while O528 was said to be oxidic in nature and related to two moieties, occupying supersurface and subsurface sites, respectively.[19] Their claim is supported by the different XPS intensity observed at normal and grazing emission. O530 was found to be unreactive towards CO and C_2H_4 oxidation and to be stable up to $T = 800$ K.

Our XPD data allow to assign both O530 and O528 on Ag(001) to adatoms: the former species sits slightly below the topmost Ag atoms on a missing-row reconstructed surface, while the latter is 0.6 Å above the fourfold hollow of the unreconstructed surface. The adsorption geometries are in agreement with the observed different chemical reactivities, as oxygen sitting in a slightly subsurface site is less accessible to adsorbed CO molecules. The decrease of the work function reported by Engelhardt and Menzel[4] upon oxygen exposure below room temperature can be explained by the combined effect of the slightly subsurface position of the oxygen (negative dipole) and by the substrate reconstruction that decreases the surface atoms density. Finally, the Ag $3d_{5/2}$ chemical core-level shift indicates that the stochiometry in the surface oxide layer is closer to Ag_2O than AgO, in agreement with the formation of Ag-O chains in the missing-row reconstructed phase. All experimental information combines therefore in a coherent picture.

When oxygen dissociation takes place below room temperature also some O528 is produced [Fig. 1(a)]. It could be observed only for grazing incidence conditions, corresponding to the largest XPS cross section for this species, and rapidly disappears after dosing, being unstable at low T. We suggest that such adatoms occupy temporarily the fourfold site between the missing rows (see Fig. 15).

The surface core-level shift of the Ag $3d_{5/2}$ peak in the presence of oxygen is independent of the adatom moiety and implies a positive charging of the Ag atoms.[52] This indicates that O528 and O530 are in the *same* oxidation state and that the shift of the O $1s$ binding energy between the two moieties results from a larger screening with positively charged Ag ions for O530. The distinction of ''oxidic'' and ''covalent'' states[18] is thus inappropriate. The screening effect is in accord with the deeper adsorption site of O530 and with the still larger binding energy observed for the subsurface species (O531) which is in contact with even more Ag ions. In agreement with this the O530 moiety forms when oxygen is coadsorbed with alkali atoms.[48]

From the experiments of Bao et al.[15] we know that O530 (O_α) is produced after extremely large oxygen doses, for which oxygen diffusion into the bulk has surely occurred.

The same is true for the study of Bukthyarov et al.,[18] who also exposed the Ag foil to atmospheric pressure. On the contrary Campbell[16,17] never observed O530 while exposed to relatively small oxygen doses. We propose therefore that a certain concentration of oxygen in the first subsurface layer (O531) is needed before conversion into O530 and substrate reconstruction become energetically favorite. O530 could accordingly exist only when stabilized by O531. The presence of this latter species is demonstrated by the binding-energy shift towards a higher value observed for the O $1s$ peak at the phase transition temperature [see Fig. 4 and Fig. 6(a)] and by the evident delay between the moment in which O530 starts to grow and the moment in which O528 starts to disappear [see 6(b)] in the reconversion process. The latter is thus triggered by the accumulation of oxygen in the immediate subsurface sites, which makes O528 unstable. The presence of oxygen dissolved in the deeper subsurface layers, on the contrary, cannot be checked directly with XPS at the photon energies available at SuperESCA. Its existence was, however, proved by Bao et al.[15] with a conventional x-ray source. We suggest that it is responsible for the stabilization of O528 on Ag(001), as the latter species did not form upon heating an O530 layer above room temperature when O_2 dosing was performed immediately after extensive surface preparation.

The proposed scenario implies that occupation of subsurface sites under the Ag atoms in the first layer takes place more easily for Ag(001) than for Ag(111) and Ag(110) for which O530 was never observed when dosing in UHV conditions. This means, for the (111) and (110) faces, either that less oxygen can migrate subsurface or that the subsurface site corresponding to O531 is not stable. The first possibility might apply to the closed-packed Ag(111) face, but it is more difficult to rationalize for the open Ag(110). However it is known that in the latter case the surface reconstructs with added O-Ag rows that might hinder subsurface migration (directly or indirectly, e.g., by impeding the diffusion of the adatoms to defect sites). Indeed, we showed some years ago that a strong disordering of Ag(110) takes place at oxygen dissociation if the crystal temperature is below the one at which the onset of the added-row reconstruction occurs.[54] Under those conditions two oxygen moieties showing very different reactivities with respect to CO oxidation could be identified by Burghaus and Conrad.[22] Surface disordering upon dissociation was not observed by scanning tunnel microscopy[55] and is therefore indicative of subsurface migration of the oxygen. The unreactive oxygen adatoms could thus correspond to O530 stabilized also in this case by subsurface oxygen in the immediate subsurface region.

In conclusion, we propose that on Ag(001) at 300 K the onset of thermal mobility of the subsurface species depletes the oxygen concentration in the immediate subsurface region, making O530 unstable. The adatoms convert then to O528. When cooling the sample segregation from the bulk towards surface and immediate subsurface region occurs, as demonstrated by the formation of O531 and by the fact that after the reconversion process the coverage Θ_{O530} can be larger than the initial value of Θ_{O528} [see 6(b)]. The occurrence of segregation to the immediate subsurface region implies that the potential well for oxygen is deeper than for bulk sites, so that at $T = 100$ K migration off it can be in-

hibited while between bulk sites it is still active. When the subsurface oxygen concentration (i.e., O531) reaches some critical value, O528 converts back to O530. Within this frame the time constant of the backconversion process would naturally depend on the subsurface oxygen content, thus explaining the different value found in the different beam times. In the second run, in fact, the subsurface concentration of oxygen is likely to have been larger than in the last one since the sample had remained several months exposed to atmospheric pressure before being inserted into the UHV chamber of the SuperESCA beam line, while in the last beam time it had been transferred directly from the UHV chamber in Genova to the one in Trieste. Typical time constants of 3000 sec were then measured for the backconversion process, to be compared with those of about 20000 sec observed in the last run.

The lower thermal stability of O530 in our experiment, compared to the one reported by Bao *et al.*[13] and Bukthyarov *et al.*,[18,19] should be related to the different concentrations of dissolved oxygen obtained when dosing in ultrahigh vacuum, as we did, and at atmospheric pressure, as done in Refs. 13,18, and 19. We can therefore be reasonably confident that our O530 coincides with the O_α of Bao *et al.*[13] and with the ''covalent'' oxygen of Bukthyarov *et al.*[18]

Finally, we would like to comment on the production of oxygen with a binding energy of 529.0 eV obtained after CO oxidation (see Fig. 18). Oxygen with such a binding energy could be produced also on Ag(111) and was associated to the formation of a surface oxide layer.[15] Such oxide was demonstrated to be active in the catalytic methanol oxidation.[56] As the (111) geometry is essential for its production, we assign our oxygen at 529 eV to the growth and oxidation of (111) microfacets at the steps oriented along the (110) direction on Ag(001). Steps along such direction have indeed the lowest energy on this surface and should be relatively abundant.

As a last experiment, we tried to run the epoxidation reaction by dosing C_2H_4 on the O530- and O528-covered Ag(001) surface in order to test the role played by these oxygen moieties in the catalytic reaction. According to Bukthyarov *et al.*[18,19] the reaction should run when both moieties are present on the surface as one is reactive, while the other stabilizes ethylene adsorption. No ethylene epoxide formation was, however, detected in our experiment independently of the relative abundance of O530 and O528 on the surface,

neither as an adsorbate by HREELS nor in the gas phase by mass spectroscopy. The reaction probability is thus estimated to be smaller than 10^{-5}. Microreactor studies estimated indeed the reaction chance to be of the order of 10^{-8} at 573 K (Ref. 57) so that no products are expected to be detectable in our experimental conditions. Our negative result indicates that, if identification of O530 with the relevant species active in partial oxidation of C_2H_4 were correct, some energy barrier must still be present, which could not be overcome in our supersonic molecular-beam experiments.

V. CONCLUSIONS

In conclusion we find that when dosing at 150 K, oxygen on Ag(001) induces a missing-row reconstruction of the substrate and forms a species characterized by an O $1s$ binding energy of 530.3 eV. Such phase is stable up to $T = 300$ K, when it starts to transform into another phase characterized by the smaller O $1s$ binding energy of 528.3 eV. Simultaneously, surface dereconstruction and oxygen dissolution into the bulk occur. Further faint peaks were observed for particular experimental conditions at $E_B(\text{O } 1s)$ of 530.9 eV and 529.0 eV and were assigned to oxygen below the first Ag layer and to a surface oxide phase on Ag(111) facets, respectively. O530 and O528 eV were investigated by HREELS, XPS (core levels and valence band), and XPD demonstrating that the phase transition implies a change in the adsorption site as well as in the chemical reactivity. The reconstructed O530 phase could be restored by cooling the sample below room temperature. The recovery time as well as the reactivity of O528 towards CO oxidation were found to depend on the history of the sample being most probably determined by its subsurface oxygen content.

*Author to whom correspondence should be addressed. FAX: +390103622790. Electronic address: Rocca@fisica.unige.it

†Present address: Physikalische Chemie I, Ruhr Universität Bochum, 44700 Bochum, Germany.

‡Also at Dipartimento di Fisica and Istituto Nazionale per la Fisica della Materia, Trieste, Italy.

[1] C.T. Campbell and M. Paffett, Surf. Sci. **139**, 396 (1984).

[2] R.A. Van Santen and H.P.C. Kuipers, Adv. Catal. **35**, 256 (1990).

[3] L. Vattuone, C. Boragno, M. Pupo, P. Restelli, M. Rocca, and U. Valbusa, Phys. Rev. Lett. **72**, 510 (1994); M. Rocca, Phys. Scr. **T66**, 202 (1996); A. Raukema and A. Kleyn, Phys. Rev. Lett. **74**, 4333 (1995); P.A. Gravil, D.M. Bird, and J.A. White, *ibid.* **77**, 3933 (1996); F. Bartolucci, R. Franchy, J.C. Barnard, and R.E. Palmer, *ibid.* **80**, 5224 (1998).

[4] H.A. Engelhardt and D. Menzel, Surf. Sci. **57**, 591 (1976).

[5] C. Backx, C.P.M. de Groot, R. Biloen, and W.M.H. Sachtler, Surf. Sci. **128**, 81 (1983); **104**, 300 (1981).

[6] F. Buatier de Mongeot, U. Valbusa, and M. Rocca, Surf. Sci. **363**, 68 (1996).

[7] F. Buatier de Mongeot, A. Cupolillo, M. Rocca, and U. Valbusa, J. Chem. Phys. **106**, 9297 (1997).

[8] F. Buatier de Mongeot, A. Cupolillo, U. Valbusa, and M. Rocca, Chem. Phys. Lett. **270**, 345 (1997).

[9] C.S. Ares Fang, Surf. Sci. **235** L291 (1990).

[10] U. Burghaus, L. Vattuone, P. Gambardella, and M. Rocca, Surf. Sci. **374**, 1 (1997).

[11] L. Vattuone, P. Gambardella, F. Cemic, U. Valbusa, and M. Rocca, Chem. Phys. Lett. **278**, 245 (1997).

[12] F. Buatier de Mongeot, A. Cupolillo, M. Rocca, and U. Valbusa, Chem. Phys. Lett. **302**, 302 (1999).

[13] B. Pettinger, X. Bao, I.C. Wilcock, M. Muhler, and G. Ertl, Phys. Rev. Lett. **72**, 1561 (1994); X. Bao, B. Pettinger, G. Ertl, and R. Schloegl, Ber. Bunsenges. Phys. Chem. **97**, 322 (1993).

[14] C. Rehren, M. Muhler, X. Bao, R. Schlögl, and G. Ertl, Z. Phys. Chem. (Munich) **174**, 11 (1991).

[15] X. Bao, M. Muhler, B. Pettinger, R. Schloegl, and G. Ertl, Catal. Lett. **22**, 215 (1993); X. Bao, M. Muhler, Th. Schedel-Niedrig, and R. Schloegl, Phys. Rev. B **54**, 2249 (1996); Th. Schedel-Niedrig, X. Bao, M. Muhler, and R. Schlögl, Ber. Bunsenges. Phys. Chem. **101**, 994 (1997).

[16] C.T. Campbell and M.T. Paffett, Surf. Sci. **143**, 517 (1984).

[17] C.T. Campbell, Surf. Sci. **157**, 43 (1985); **173**, L641 (1986).

[18] V.I. Bukhtyarov, A.I. Boronin, and V.I. Savchenko, J. Catal. **150**, 262 (1994).

[19] A.I. Boronin, A.L. Vishnevskii, G.K. Boreskov, and V.I. Savchenko, Surf. Sci. **201**, 195 (1988).

[20] V.I. Bukhtyarov, A.I. Boronin, and V.I. Savchenko, Surf. Sci. Lett. **232**, L205 (1994).

[21] V.I. Bukhtyarov, A.I. Boronin, I.P. Prosvirin, and V.I. Savchenko, J. Catal. **150**, 268 (1994).

[22] U. Burghaus and H. Conrad, Surf. Sci. **370**, 17 (1997); **331-333**, 116 (1995).

[23] M. Rocca, U. Valbusa, A. Gussoni, G. Maloberti, and L. Racca, Rev. Sci. Instrum. **62**, 2172 (1991).

[24] M. Rocca, P. Traversaro, and U. Valbusa, J. Electron Spectrosc. Relat. Phenom. **54/55**, 131 (1990).

[25] A. Abrami, M. Barnaba, L. Battistello, A. Bianco, B. Brena, *et al.*, Rev. Sci. Instrum. **66**, 1618 (1995).

[26] J.F. Weaver and G.B. Hoflund, J. Phys. Chem. **98**, 8519 (1994).

[27] P.H. Citrin, G.K. Wertheim, and Y. Baer, Phys. Rev. B **27**, 3160 (1983).

[28] J.N. Andersen, D. Henning, E. Lundgren, M. Mathfessel, R. Nyholm, and M. Scheffler, Phys. Rev. B **50**, 17 525 (1994).

[29] L. Vattuone, U. Valbusa, and M. Rocca, Surf. Sci. **369**, 336 (1996).

[30] F. Buatier de Mongeot, A. Cupolillo, M. Rocca, U. Valbusa, J. Kreuzer, and S.H. Payne, J. Chem. Phys. **106**, 711 (1997).

[31] S.L. Qiu, C.L. Lin, J. Chen, and M. Strongin, Phys. Rev. B **41**, 7467 (1990).

[32] L. Vattuone, P. Gambardella, M. Rocca, and U. Valbusa, Surf. Sci. **377/379**, 671 (1997).

[33] R. Mayer, Chun-Si Zhang, and K.G. Lynn, Phys. Rev. B **33**, 8899 (1986).

[34] M. Wuttig, R. Franchy, and H. Ibach, Surf. Sci. **213**, 103 (1989).

[35] F.M. Leibsle, Surf. Sci. **337**, 51 (1995); F. Jensen, F. Besenbacher, E. Laegsgaard, and I. Stensgaard, Phys. Rev. B **42**, 9206 (1990).

[36] M.J. Braithwaite, R.W. Joyner, and M.W. Roberts, Faraday Discuss. Chem. Soc. **60**, 89 (1975).

[37] M.C. Asensio, M.J. Ashwin, A.L.D. Kilcoyne, D.P. Woodruff, A.W. Robinson, Th. Lindner, J.S. Somers, D.E. Ricken, and A.M. Bradshaw, Surf. Sci. **236**, 1 (1990).

[38] M. Rocca, Surf. Sci. Rep. **22**, 1 (1995).

[39] L.H. Tjeng, M.B. Meinders, and G.A. Sawatzky, Surf. Sci. **223**, 341 (1990).

[40] T.E. Felter, W.H. Weinberg, G.Ya. Lastushkina, A.I. Boronin, P.A. Zhdan, G.K. Boreskov, and J. Hrbek, Surf. Sci. **118**, 369 (1982).

[41] J.S. Hammond, S.W. Gaarenstroom, and N. Winograd, Anal. Chem. **47**, 2193 (1975).

[42] If the atomic oxygen moiety vibrating at 30 meV were produced also for large exposures at $T=100$ K, one could satisfactorily explain the anomalous behavior of the intensity of the 30-meV loss with O_2 coverage (Ref. 7).

[43] C. S. Fadley, in *Synchrotron Radiation Research: Advances in Surface Science*, edited by Z. Bachrach (Plenum Press, New York, 1990).

[44] D. Agliz, A. Quémerais, and D. Sébilleau, Surf. Sci. **343**, 80 (1995).

[45] R. Gunnella, E.L. Bullock, L. Patthey, C.R. Natoli, T. Abukawa, S. Kono, and L.S.O. Johansson, Phys. Rev. B **57**, 14 739 (1998).

[46] R. Gunnella, F. Solal, and C. R. Natoli (unpublished).

[47] C.S. Fadley, Prog. Surf. Sci. **16**, 275 (1984). The correction was not applied to the O530 data as the effect is less important for a subsurface species.

[48] M. Ayyoob and M.S. Hedge, Surf. Sci. **133**, 516 (1983).

[49] J. Eickmans, A. Otto, and A. Goldmann, Surf. Sci. **149**, 293 (1985); J. Eickmans, A. Goldmann, and A. Otto, *ibid.* **127**, 153 (1983).

[50] R.W. Joyner and M.W. Roberts, Chem. Phys. Lett. **60**, 459 (1979); R.W. Joyner, Surf. Sci. **63**, 291 (1977).

[51] D.A. Outka, J. Stöhr, W. Jark, P. Stevens, J. Salomon, and R.J. Madix, Phys. Rev. B **35**, 4119 (1987).

[52] G. Benedek, F. Buatier de Mongeot, U. Valbusa, and M. Rocca (unpublished).

[53] L.H. Tjeng, M.B.J. Meinders, J. van Elp, J. Ghjisen, G.A. Sawatzky, and R.L. Johnsen, Phys. Rev. B **41**, 3190 (1990).

[54] L. Vattuone, M. Rocca, P. Restelli, M. Pupo, C. Boragno, and U. Valbusa, Phys. Rev. B **49**, 5113 (1994).

[55] J. Wintterlin (private communication).

[56] X. Bao, M. Muhler, B. Pettinger, R. Schloegl, and G. Ertl, Catal. Lett. **22**, 215 (1993).

[57] C. Backx, J. Moolhuysen, P. Geenen, and R.A. Van Santen, J. Catal. **72**, 364 (1981).